Springer

KSME

Journal of Mechanical Science and Technology 29 (1) (2015) 269~278
www.springerlink.com/content/1738-494x
DOI 10.1007/s12206-014-1233-9

Two-step design process for optimal suction muffler in reciprocating compressor †

Kee Seung Oh and Jin Woo Lee*

Division of Mechanical Engineering, Ajou University, 206, World cup-ro, Yeongtong-Gu, Suwon, 443-749, Korea

(Manuscript Received December 6, 2013; Revised June 26, 2014; Accepted September 3, 2014)

Abstract

A systematic design process for an optimal suction muffler is proposed to reduce the noise of a reciprocating compressor. Because the outer shape of a suction muffler is complicated, the well-known internal configuration for simple expansion chamber mufflers is not easily applicable to the suction muffler design problem. To achieve an optimal design of a suction muffler, two sequential optimization problems are formulated to maximize the transmission loss value at a target frequency: acoustical topology and shape optimization problems. The key idea in the suggested method is to use an optimal topology obtained by solving the topology optimization problem as an initial shape for the shape optimization problem. The formulated optimization problems are solved at several target frequencies, and the acoustical characteristics of the optimal shapes are closely investigated. The experimental results for two optimal suction mufflers support the validity of our suggested two-step design process for optimal suction mufflers.

Keywords: Optimal design; Reciprocating compressor; Shape optimization; Suction muffler; Topology optimization; Transmission loss

1. Introduction

A suction muffler is installed between an intake pipe and a suction port in a reciprocating compressor to reduce the noise generated by the pressure pulsation of the inflow refrigerant or the impact of a suction valve [1-3]. To increase the transmission loss value in the dominant frequency range of the noise, the geometry of a suction muffler, including its outer shape and internal configuration, and its inlet and outlet locations must be carefully determined. However, because the location and volume of a suction muffler generally have low priorities during the development of a new reciprocating compressor with a high energy efficiency, the outer shape of a suction muffler is generally irregular or complicated, and its inlet and outlet locations are determined without considering noise reduction. Therefore, the internal configuration of a suction muffler should be effectively designed to reduce the noise caused by the inflow refrigerant.

The conventional design strategy is the insertion of rigid partitions to form several separate chambers or resonators inside a suction muffler to increase the transmission loss value in a target frequency range. Lee et al. [4] divided a suction muffler into several chambers. Svendsen and Møller [5] divided a suction muffler into a lower chamber and an upper chamber with inserted partitions. Gosavi et al. [6] evaluated the effect of the geometry of the inserted tube on the transmission loss characteristics of a suction muffler. While general methods to determine the optimal location and length of the inserted partitions have already been reported for a simple expansion chamber muffler [7-12], a systematic design method for an optimal suction muffler has not yet been introduced because of its irregular outer shape.

In an attempt to optimally design a suction muffler, acoustical shape optimization problems were formulated and solved by using the sequential quadratic programming method and Taguchi's method [5, 6]. The transmission loss values of the obtained optimal mufflers were dramatically increased in a target frequency range. Moreover, the optimal shape obtained was not difficult to manufacture. However, a shape optimization-based design method strongly depends on the initial shape. A good initial shape should be selected for a good optimal result. Usually, a good initial shape requires a large amount of efforts by a very experienced designer.

Since Bendsøe and Kikuchi [13] successfully applied topology optimization using computer-based simulation to structural design problems, the topology optimization design method has been used in various applications [14]. Recently, Lee et al. [15-17] introduced a muffler design method that used topology optimization. They showed the possibility of using this topology optimization-based muffler design method to obtain a creatively designed internal configuration for a simple expansion chamber muffler. However, their approach is open to further improvements in relation to the designing and manufacturing real mufflers because, even at the same target frequency, the optimal topology is strongly affected by

*Corresponding author. Tel.: +82 31 219 3659, Fax.: +82 31 219 1611
E-mail address: jinwoolee@ajou.ac.kr
† Recommended by Associate Editor Gang-Won Jang

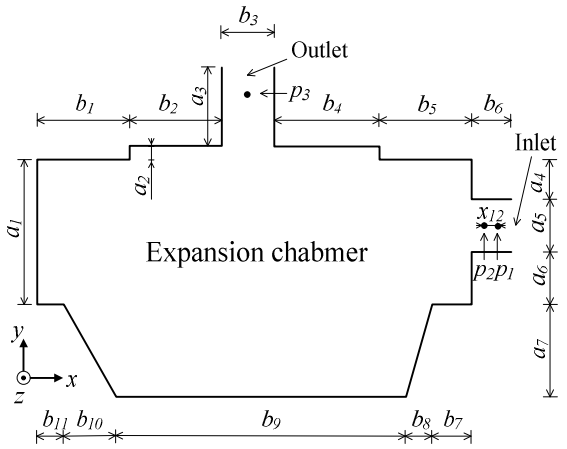

Fig. 1. Suction muffler, where refrigerant enters from right end (inlet) and leaves through top end (outlet).

the allowed rigid partition volume ratio, and some optimal topologies are difficult to manufacture in industry.

In this paper, we propose a two-step design process for an optimal suction muffler, which combines the advantages of topology optimization and shape optimization. The suggested design process is validated by experiments on optimized suction mufflers. To that end, two separate optimization problems are formulated: an acoustical topology optimization problem and an acoustical shape optimization problem with the same objective function. This suggested design process has the advantage of using one optimization method to overcome the shortcomings of the other. The finite element method and a gradient-based optimization scheme are employed. Optimal topologies will be used as the initial shape in the acoustical shape optimization problem. Design variables are used to determine the acoustical properties of each finite element, and the total volume of the rigid partitions are constrained in the acoustical topology optimization problem. The lengths of the partitions are selected as design variables, which are constrained in the acoustical shape optimization problem. Two optimal acrylic mufflers are constructed in the experiment, and the measured transmission loss curves are compared with those of optimal finite element models. All of the numerical solutions are obtained by using COMSOL multiphysics (versions 3.5 and 4.3) and MATLAB.

2. Optimization problem setup for optimal suction muffler

Two acoustical optimization problems are formulated for an optimal suction muffler, as shown in Fig. 1, where the outer shape comes from the suction muffler in Ref. [5]. Because the exact dimensions were not provided in the reference, the lengths of all the sides are properly scaled. The depth (z-direction) of an expansion chamber of the suction muffler in Fig. 1 is assumed to be equal to the depths of its inlet and outlet. Compared with the width and height of the expansion chamber, its depth is so small that the muffler could be assumed to be a two-dimensional acoustical device in an acoustical topology optimization problem [18].

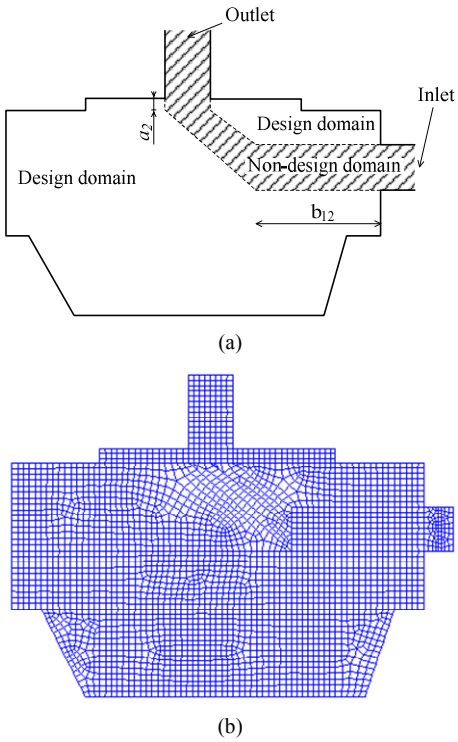

Fig. 2. Analysis model: (a) design domain and non-design domain; (b) finite element model.

2.1 First step: acoustical topology optimization problem

The transmission loss values (TL) at target frequencies (f_t) are multiplied by their respective weighting factors (w_t), and the sum of the values thus obtained is selected as the objective function in Eq. (1). The total volume of the rigid partitions is constrained, as indicated in Eq. (2). The expansion chamber is divided into a design domain and a non-design domain for fluid passage, as shown in Fig. 2(a).

$$\min_{\boldsymbol{\chi}} -\sum_{t=1}^{T} w_t \cdot TL\left(f_t;\boldsymbol{\chi}\right) \tag{1}$$

$$\left(\int_V \boldsymbol{\chi}(r)dV\right)/V \le V_a \tag{2}$$

where T is the total number of target frequencies and $\boldsymbol{\chi}$ represents the design variables, which are functions of r. The variable r represents the position ($r=(x,y)$ in a two-dimensional space and $r=(x,y,z)$ in a three-dimensional space), and V_a represents the ratio between the volume of the allowed rigid partitions and the total volume (V) of the design domain.

The finite element model shown in Fig. 2(b) is used for an acoustical analysis. All the elements in the non-design domain are filled with fluid, but the density and bulk modulus of each element in the design domain are determined by the associated

design variables χ, which change continuously from "0" to "1" during the optimization process. The associated element for $\chi = 0$ is filled with a fluid element, and an incident acoustic wave is freely transmitted to the other side. In contrast, one element for $\chi = 1$ is filled with a rigid element, and an incident acoustic wave is fully reflected. The rigid elements build up rigid partitions. To ensure that all the design variables become "0" or "1" when the objective function converges, carefully-selected functions are used in Eq. (3) as interpolation functions of the design variables that were validated in previous studies [15-17].

$$1/\rho(\chi) = 1/\rho_{\text{fluid}} + \chi\left(1/\rho_{\text{rigid}} - 1/\rho_{\text{fluid}}\right) \tag{3a}$$

$$1/K(\chi) = 1/K_{\text{fluid}} + \chi\left(1/K_{\text{rigid}} - 1/K_{\text{fluid}}\right) \tag{3b}$$

where the subscripts "fluid" and "rigid" represent fluid and rigid elements, respectively, and ρ and K represent the density and bulk modulus ($K = \rho c^2$, c is the speed of sound in the acoustic medium), respectively.

The transmission loss value at a target frequency is calculated by using the three-point method [19], as expressed in Eq. (4). The acoustic pressures (p_1, p_2, p_3) at three points, whose locations are illustrated in Fig. 1, are obtained by solving the Helmholtz equation for acoustic pressure in Eq. (5) with the finite element model, as shown in Fig. 2(b). Eq. (6) represents the relationship between the acoustic pressure (p) and the particle velocity (u). The particle velocity of a unit magnitude in Eq. (7a) is assigned to the inlet end, the anechoic termination condition in Eq. (7b) is assigned to the outlet end, and rigid wall condition in Eq. (7c) is assigned to other boundaries.

$$TL(f;\chi) = 20 \cdot \log_{10}\left|\frac{p_{in}}{p_{out}}\right|, \quad j = \sqrt{-1}, \quad k = \frac{2\pi f}{c} \tag{4a}$$

$$\left|p_{\text{in}}\right| = \left|\left(p_1 - p_2 \cdot e^{-jk\cdot x_{12}}\right)/\left(1 - e^{-j2k\cdot x_{12}}\right)\right| \tag{4b}$$

$$\left|p_{\text{out}}\right| = \left|p_3\right| \tag{4c}$$

where x_{12} represents the distance between two points in the inlet and f is the frequency.

$$\nabla\cdot\left(\frac{1}{\rho}\nabla p\right) + \frac{\omega^2}{K}p = 0 \tag{5}$$

where ω is the angular frequency ($\omega = 2\pi f$).

$$u = -\frac{1}{j\rho\omega}\cdot\nabla p \tag{6}$$

$$u = 1 \quad \text{for an inlet boundary} \tag{7a}$$

$$p/u = \rho c \quad \text{for an outlet boundary} \tag{7b}$$

$$u = 0 \quad \text{for other boundaries.} \tag{7c}$$

As a gradient-based optimizer, the method of moving asymptotes [20] is used to update the design variables. This requires the sensitivity analysis of the objective function in Eq. (1) with respect to each design variable [15]:

$$\frac{dTL(f_t;\boldsymbol{\chi})}{d\chi} = \frac{10}{\ln 10}\cdot\left(\frac{1}{\left|p_{\text{in}}\right|^2}\cdot\frac{\partial\left|p_{\text{in}}\right|^2}{\partial\chi} - \frac{1}{\left|p_{\text{out}}\right|^2}\cdot\frac{\partial\left|p_{\text{out}}\right|^2}{\partial\chi}\right) \tag{8}$$

where the symbol "ln" denotes the natural logarithm.

2.2 Second step: acoustical shape optimization problem

An acoustical shape optimization problem is formulated using the objective function in Eq. (9) and constraints in Eq. (10) for an initial partition configuration inside the expansion chamber of a suction muffler. An optimal topology obtained by solving the acoustical topology optimization problem formulated in the previous section will be used as an initial partition configuration in which one design variable (l_n) is assigned to each partition. Unlike in the case of Eq. (2) where the partition volume was constrained, the lengths of the partitions are constrained as in Eq. (10)

$$\min_{l_n} -\sum_{t=1}^{T} w_t \cdot TL(f_t;l_n) \tag{9}$$

$$l_n^{lower} \le l_n \le l_n^{upper}, \ (n = 1,2,\cdots,N) \tag{10}$$

where l_n^{lower} and l_n^{upper} represent the lower and upper limit values of each design variable (l_n), respectively, and N is the total number of design variables. Because all the elements are filled with fluid in the shape optimization problem, the interpolation function in Eq. (3) is not required. For an updated finite element model of a suction muffler with partitions at each iterative calculation, the acoustic pressures at the three points shown in Fig. 1 are calculated by using Eqs. (5)-(7), and the transmission loss values at the target frequencies are calculated by using the three-point method [19] during the optimization process. For a sensitivity analysis, the gradient of the objective function shown in Eq. (9) with respect to the design variable (l_n) is calculated by using the following difference equation:

$$\frac{\partial TL(f_t;l_n)}{\partial l_n} \cong \frac{TL(f_t;l_n + \Delta l_n) - TL(f_t;l_n)}{\Delta l_n}. \tag{11}$$

3. Numerical results

The two acoustical optimization problems formulated in the previous section are sequentially solved by following the flow charts shown in Fig. 3. The iteration calculation is stopped when the difference between the current and previous objective functions are less than 10^{-4}. First, the acoustical topology optimization problem is solved using the first flow chart shown in Fig. 3(a) at several target frequencies and volume

Table 1. Geometrical information for suction muffler used in solving optimization problems.

Symbol	Value	Symbol	Value	Symbol	Value
a_1	0.050 m	b_1	0.030 m	b_7	0.010 m
a_2	0.005 m	b_2	0.030 m	b_8	0.010 m
a_3	0.025 m	b_3	0.015 m	b_9	0.095 m
a_4	0.015 m	b_4	0.035 m	b_{10}	0.015 m
a_5	0.015 m	b_5	0.030 m	b_{11}	0.010 m
a_6	0.020 m	b_6	0.010 m	b_{12}	0.045 m
a_7	0.030 m				

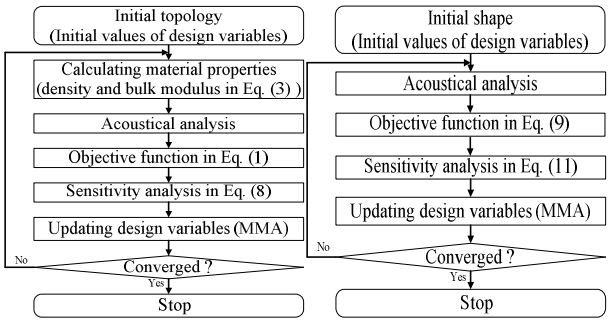

(a) (b)

Fig. 3. Flow charts for solving optimization problems formulated for suggested muffler design method: (a) acoustical topology optimization problem; (b) acoustical shape optimization problem.

ratios. Second, the acoustical shape optimization problem is solved using the second flow chart shown in Fig. 3(b) and the initial shape, which is determined on the basis of the obtained optimal topologies. To carry out acoustical analysis for two optimization problems, the standard finite element method is employed: Eqs. (5)-(7) are converted to the finite element approximation shown in Eq. (12):

$$\left[\mathbf{K} - \omega^2 \mathbf{M}\right]\mathbf{P} = \mathbf{F} \tag{12}$$

where **K** and **M** are the stiffness matrix and the mass matrix, respectively, and **P** and **F** are the nodal vectors of the acoustic pressure and equivalent force, which are the functions of shape functions and acoustical properties expressed in Refs. [15-17]. Numerical calculations and design variable updating are carried out by using the Partial Differential Equation module of COMSOL Multiphysics (versions 3.5 and 4.3) with MATLAB [17, 21, 22] and a gradient-based optimization algorithm, MMA [20]. The geometrical information of the suction muffler shown in Figs. 1 and 2(a) is summarized in Table 1. The values of the variables used in the optimization problems are specified in Table 2. The fluid in the optimization problem is assumed to be air. The density and sound speed values of a rigid body element are determined using the criteria suggested in Ref. [23].

Table 2. Specific values of symbols used for optimization problems.

Symbols	Quantity	Value
x_{12}	Distance between two measurement points in the inlet	0.001 m
ρ_{fluid}	Density of fluid	1.21 kg/m^3
c_{fluid}	Sound speed in fluid	343 m/s
ρ_{rigid}	Density of a rigid body	$10^7 \cdot \rho_{\text{fluid}}$
c_{rigid}	Sound speed in a rigid body	$10^1 \cdot c_{\text{fluid}}$
l_1^{upper}	Upper limit value of design variable l_1	0.085 m
l_1^{lower}	Lower limit value of design variable l_1	0.001 m
l_2^{upper}	Upper limit value of design variable l_2	0.06 m
l_2^{lower}	Lower limit value of design variable l_2	0.001 m
l_3^{upper}	Upper limit value of design variable l_3	0.04 m
l_3^{lower}	Lower limit value of design variable l_3	0.001 m

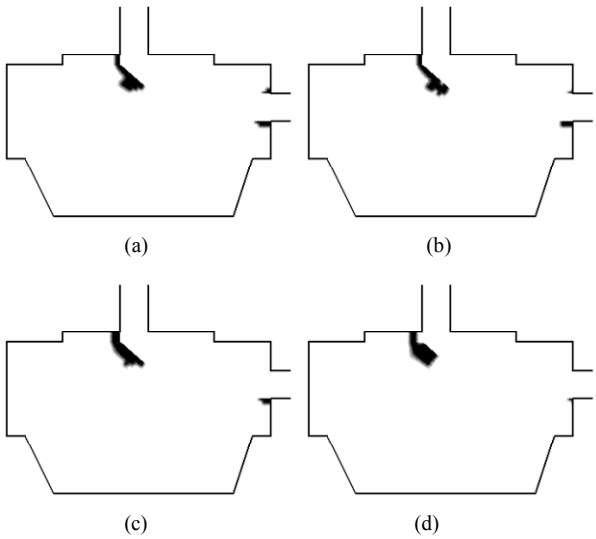

(a) (b) (c) (d)

Fig. 4. Optimal topologies depending on target frequency for $V_a = 0.015$: (a) $f_t = 400$ Hz ; (b) $f_t = 600$ Hz ; (c) $f_t = 800$ Hz ; (d) $f_t = 1000$ Hz .

3.1 Optimal topologies

3.1.1 Single target frequency

For $V_a = 0.015$, the acoustical topology optimization formulated in Eqs. (1)-(3) is solved at four single target frequencies: $f_t = 400$ Hz, 600 Hz, 800 Hz, 1000 Hz. The initial values of the design variables are set to zero. Fig. 4 shows the optimal topologies at the target frequencies. While the white areas represent fluid elements, the black areas represent rigid body elements, which build up the partitions. The locations of the partitions are strongly affected by the target frequency. In the optimal topology at 400 Hz, three partitions are built up along the board between the design domain and the non-design domain: two partitions around the inlet and the other partition around the outlet. As the target frequency increases, the width of the partition around the outlet increases, and the lengths of the two partitions around the inlet decrease. In the optimal

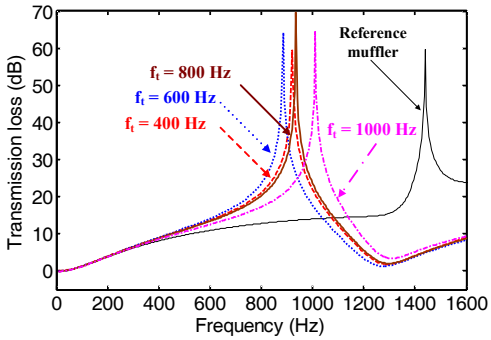

Fig. 5. Comparison of transmission loss curves of optimal topologies in Fig. 4 and reference muffler.

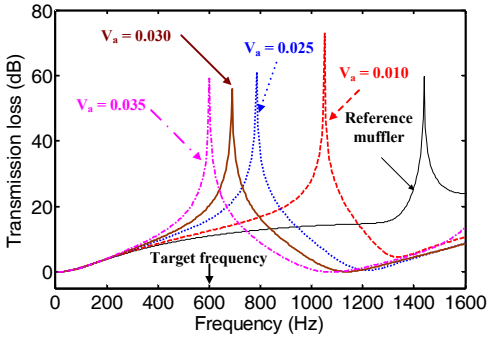

Fig. 7. Comparison of transmission loss curves of optimal topologies in Fig. 6 and reference muffler.

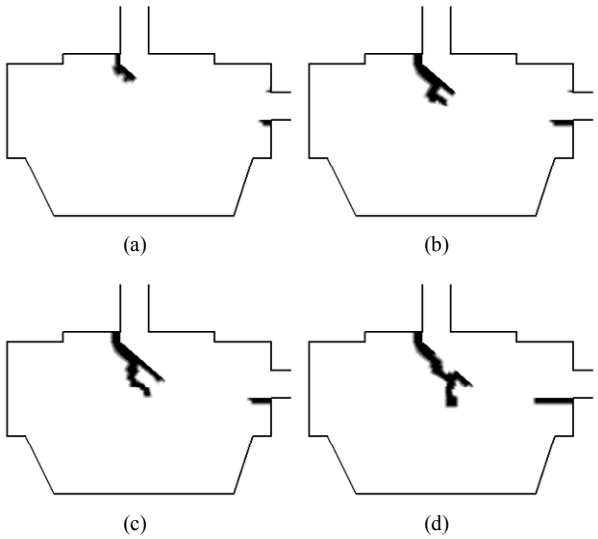

Fig. 6. Optimal topologies depending on volume ratio of partitions at $f_t = 600$ Hz : (a) $V_a = 0.010$; (b) $V_a = 0.025$; (c) $V_a = 0.030$; (d) $V_a = 0.035$.

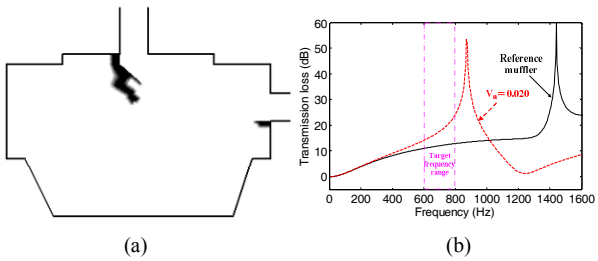

Fig. 8. Optimal results obtained at multiple target frequencies ($f_t = 600$ Hz , 650 Hz , 700 Hz , 750 Hz , 800 Hz) for $V_a = 0.020$: (a) optimal topology; (b) comparison of transmission loss curves of optimal topology and reference muffler.

topology at 1000 Hz (Fig. 4(d)), one thick and short partition is located around the outlet, and one short partition is placed around the inlet.

Fig. 5 compares the transmission loss curves of the optimal topologies shown in Fig. 4 with the transmission loss curve of the reference muffler, where all elements are filled with fluid. The transmission loss values of the reference muffler at the target frequencies are 8.12 dB at 400 Hz, 10.95 dB at 600 Hz, 12.83 dB at 800 Hz, and 14.02 dB at 1000 Hz. The transmission loss value of the optimal topology obtained at each target frequency is increased by 0.86-26.18 dB: the improvements of the optimal topologies are 0.86 dB at 400 Hz, 3.19 dB at 600 Hz, 7.49 dB at 800 Hz, and 26.18 dB at 1000 Hz.

To investigate the effect of the volume ratio (V_a) on the optimal topologies, the formulated topology optimization problem is solved at 600 Hz for four volume ratios: $V_a = 0.010,\ 0.025,\ 0.030,\ 0.035$. Fig. 6 compares the dependences of the four optimal topologies on the volume ratio. As shown in Fig. 6(a), one partition is placed around the outlet, and one shorter upper partition and one longer lower partition are placed around the inlet in the optimal topology for $V_a = 0.010$. As the volume ratio increases, the end of the partition around the outlet is divided into two branches; the lower partition around the inlet is lengthened, and the upper partition around the inlet almost vanishes. The transmission loss value at the target frequency dramatically increases with the volume ratio, as shown in Fig. 7.

3.1.2 Multiple target frequencies

To improve the acoustical attenuation performance of the suction muffler in a wider frequency range, the transmission loss values at multiple target frequencies are maximized. Two cases are considered, depending on the target frequency range and the volume ratio. In Case 1, five equidistant frequencies from 600 Hz to 800 Hz are used as target frequencies (600 Hz, 650 Hz, 700 Hz, 750 Hz, and 800 Hz) for $V_a = 0.020$. Fig. 8 shows the optimal results obtained with equivalent weighting factors. The optimal topology shown in Fig. 8(a) looks similar to the optimal topology shown in Fig. 6(b), which was obtained at 600 Hz for $V_a = 0.025$, but the lower branch of the partition around the outlet has been thickened to improve the transmission loss values at the other target frequencies, as shown in Fig. 8(b). In Case 2, the transmission loss values at 800 Hz, 850 Hz, 900 Hz, 950 Hz, and 1000 Hz are maximized simultaneously with the same weighting factors for 10 volume

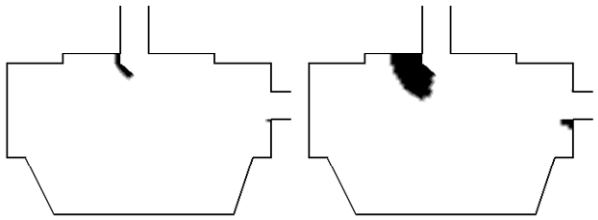

Fig. 9. Optimal topologies at multiple target frequencies (f_t = 800 Hz , 850 Hz , 900 Hz , 950 Hz , 1000 Hz): (a) V_a = 0.005 ; (b) V_a = 0.050 .

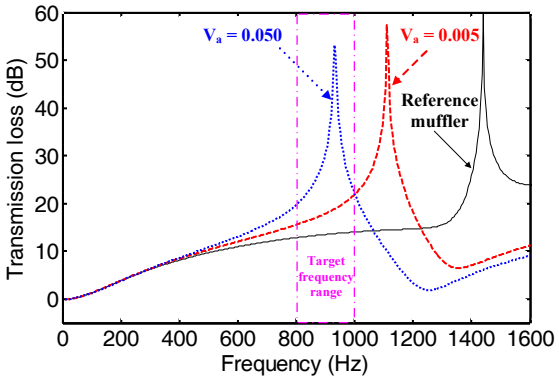

Fig. 10. Comparison of transmission loss curves of optimal topologies in Fig. 9 and reference muffler.

ratios (V_a = 0.005 ~ 0.050). Fig. 9 shows the optimal topologies for V_a = 0.005 and V_a = 0.050 , and Fig. 10 compares their transmission loss curves with that of the reference suction muffler. In Fig. 9(a), two partitions are built up around the inlet and the outlet. The widths and lengths of the two partitions increase with the volume ratio. To maximize the transmission loss values in the target frequency range, the partition around the outlet is made thicker, as shown in Fig. 9(b).

In summary, the topology optimization-based muffler design approach could successfully give an optimal topology depending on a selected target frequency for the high transmission loss of a suction muffler, as shown in Figs. 4 and 8(a). Without the topology optimization, such a creatively designed internal configuration in a suction muffler could not be easily obtained. However, even at the same target frequency, an optimal topology is strongly affected by the pre-determined volume ratio (V_a) of the partitions, as shown in Figs. 6 and 9. The peak frequency in the transmission loss curve of some optimal topologies does not coincide with the target frequency, as shown in Figs. 5 and 8(b). Moreover, some of the optimal topologies are difficult to manufacture because the partitions are non-uniform or too thick, as shown in Fig. 9(b), and their shapes are complicated, as shown in Figs. 6(b)-(d) and 8(a). Therefore, the practical implementation of the topology optimization-based design method for an optimal suction muffler requires the second step (shape optimization) formulated in Sec. 2.2.

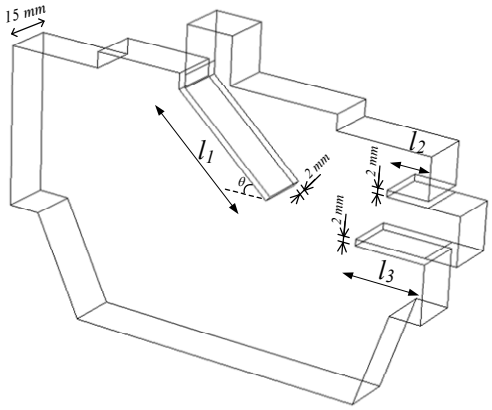

Fig. 11. Initial shape used in acoustical shape optimization problem.

3.2 Optimal shapes

3.2.1 Initial shape

Based on the optimal results obtained by solving the acoustical topology optimization problem, a good initial shape, as shown in Fig. 11, is determined for the acoustical shape optimization problem formulated in Sec. 2.2. The depth of the suction muffler is set to 15 mm for the three-dimensional design. The optimal topologies obtained in Sec. 3.1 give some information on the number of partitions and the approximate locations and lengths of the partitions: two partitions around the inlet and one partition around the outlet. The partitions are located in the board between the non-design domain and the design domain, as shown in Fig. 2(a). Considering the fact that thin and uniform partitions are generally used in the suction muffler for a commercial reciprocating compressor, the width of the partitions is set to 2 mm, even if the widths of partitions are too thick in some optimal topologies. Three design variables (l_1, l_2, l_3) are assigned to the lengths of the three partitions and constrained to prevent interference among the partitions by using Eq. (10), where the specific values are summarized in Table 2. The inclination angle θ of the partition around the outlet is set to $\theta = \arctan((a_1 - a_6) / (b_3 + b_4 + b_5 - b_{12}))$.

3.2.2 Optimal internal configuration

The acoustical shape optimization problem in Eqs. (9) and (10) is solved at three single target frequencies: f_t = 600 Hz , f_t = 800 Hz , and f_t = 1000 Hz . Fig. 12 shows the optimal internal configuration with the acoustic pressure distribution at each target frequency, where the colors represent the absolute value of the acoustic pressure. Fig. 13 compares the transmission loss curves of the optimal suction mufflers with that of the three-dimensional reference muffler. Table 3 summarizes the optimal values of the design variables. Fig. 14 compares the history of the design variables with that of the objective function during the optimization process at f_t = 1000 Hz . The transmission loss value and the absolute value of the acoustic pressure are compared at each target frequency. The comparison leads to the conclusion that an internal partition configura-

Table 3. Specific values of symbols used for optimization problems.

Figure number	Target frequency	l_1^{opt}	l_2^{opt}	l_3^{opt}
Fig. 12(a)	600 Hz	0.0441 m	0.0034 m	0.0175 m
Fig. 12(b)	800 Hz	0.0287 m	0.0025 m	0.0085 m
Fig. 12(c)	1000 Hz	0.0166 m	0.029 m	0.0100 m
Fig. 15(a)	800, 850, 900, 950, 1000 Hz	0.0184 m	0.0012 m	0.0105 m
Fig. 16(c)	400 Hz	0.0716 m	0.0039 m	0.0127 m
Fig. 16(d)	600, 650, 700, 750, 800 Hz	0.03 m	0.0014 m	0.0182 m

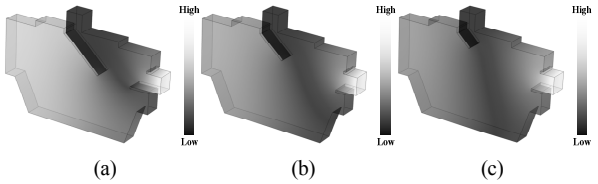

Fig. 12. Optimal shapes at three single target frequencies: (a) optimal shape at $f_t = 600$ Hz ; (b) optimal shape at $f_t = 800$ Hz ; (c) optimal shape at $f_t = 1000$ Hz .

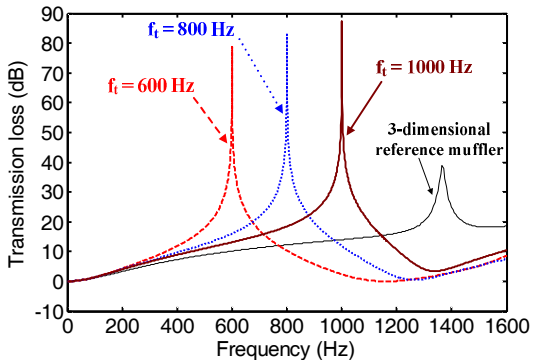

Fig. 13. Transmission loss curves of optimal shapes in Fig. 12 and three-dimensional reference muffler.

tion should be designed to minimize the absolute value of the acoustic pressure around the outlet to achieve a high transmission loss value at a target frequency. The optimal shape shown in Fig. 15(a) is successfully obtained at multiple target frequencies ($f_t = 800, 850, 900, 950, 1000$ Hz) with high transmission loss values, as shown in Fig. 15(b).

The shortcomings of the previously discussed topology optimization are eliminated by using the shape optimization. The peak frequencies in the transmission loss curves coincide with the target frequencies of optimal suction mufflers, as shown in Fig. 13. The partition volume is automatically optimized because the lengths of the partitions are optimized, and all of the optimal shapes are simple to manufacture, as shown in Figs. 12 and 15(a). The good initial shape obtained through the topology optimization was the starting point of all these results.

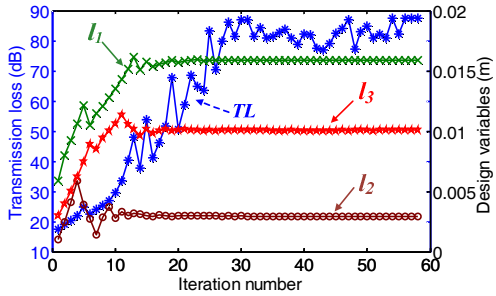

Fig. 14. History of design variables and objective function during shape optimization process at $f_t = 1000$ Hz .

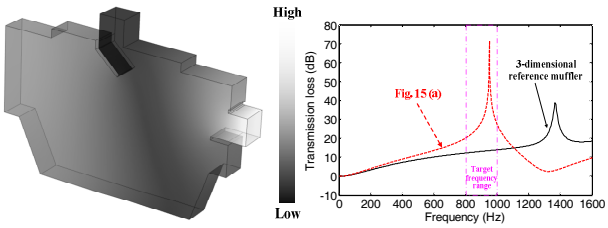

Fig. 15. Optimal results obtained at multiple target frequencies: (a) optimal shape; (b) transmission loss curve.

4. Experimental validation and summary of suggested method

To validate the suggested method experimentally, the two real acrylic mufflers shown in Figs. 16(a) and (b) were made using the optimal shapes shown in Figs. 16(c) and (d), which were obtained at a single target frequency ($f_t = 400$ Hz) and at multiple target frequencies ($f_t = 600$, 650 , 700 , 750 , 800 Hz), respectively. The experimental setup shown in Fig. 17 was used to measure the transmission loss curves of these two acrylic mufflers. The sound transmission loss module in at the LMS Test Lab, which is based on the four-microphone method, was used with four microphones (GRAS 46BE Microphone) and one horn driver (InterM DU-75). The burst random signal generated by LMS SCADAS mobile recorder was fed into the horn driver. The transmission loss curve was obtained by measuring three acoustic transfer functions with respect to microphone 3 simultaneously. The measured transmission loss curves were averaged 50 times, and their frequency resolution was 1.5625 Hz. Fig. 18 compares the measured transmission loss curves of the optimal acrylic mufflers with the calculated transmission loss curves of the optimal shapes: the suction mufflers of Figs. 16(a) and (c) in Fig. 18(a); and the suction mufflers of Figs. 16(b) and (d) in Fig. 18(b). The measured transmission loss curve in each comparison agrees well with the calculated transmission loss curve around the target frequency.

These experimental results show that our suggested muffler design approach (two-step design process) can be successfully applied to acoustical design problems involving arbitrarily-

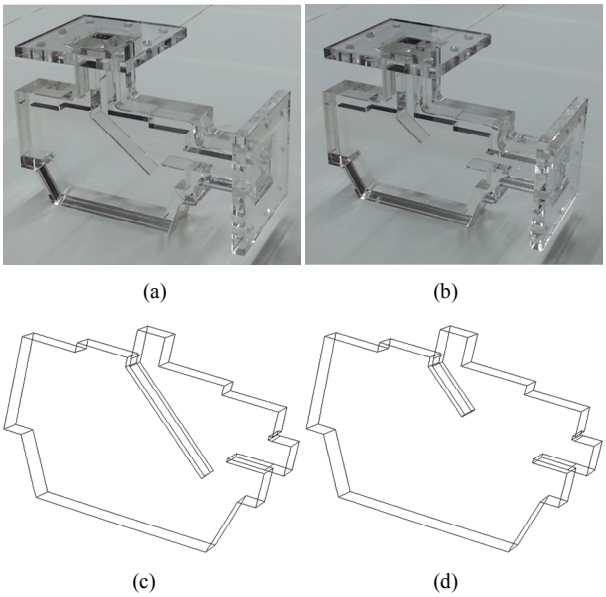

Fig. 16. Optimal shapes and acrylic mufflers used for experiment: (a) acrylic optimal muffler at 400 Hz; (b) acrylic optimal muffler at multiple target frequencies (f_t = 600 Hz , 650 Hz , 700 Hz , 750 Hz , 800 Hz); (c) optimal shape at single target frequency (400 Hz); (d) optimal shape at multiple target frequencies (f_t = 600 Hz , 650 Hz , 700 Hz , 750 Hz , 800 Hz).

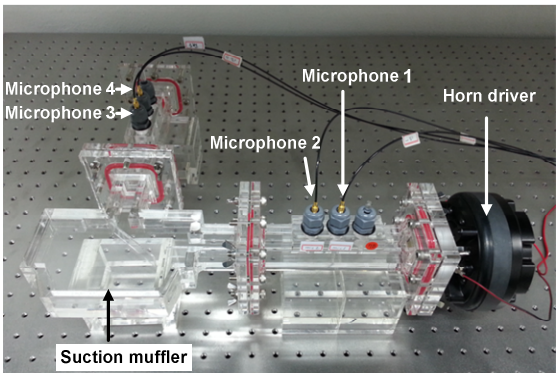

Fig. 17. Experimental setup for transmission loss measurement.

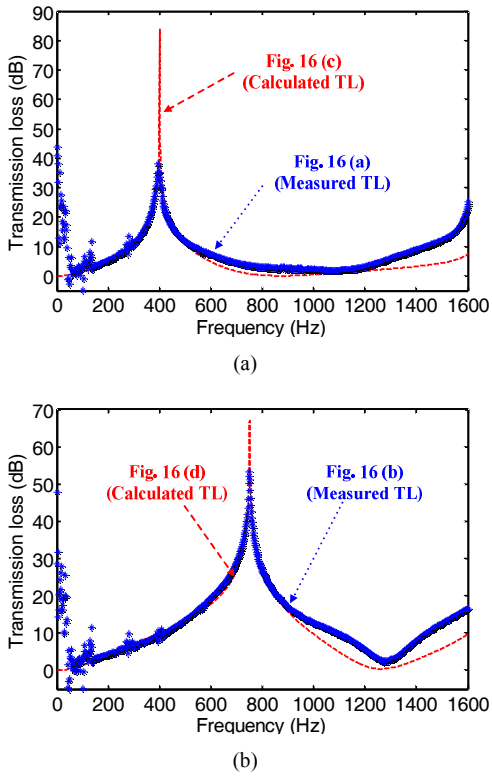

Fig. 18. Comparison of measured transmission loss curves of acrylic optimal mufflers and calculated transmission loss curves of optimal finite element models: (a) single target frequency (400 Hz); (b) multiple target frequencies (f_t = 600 , 650 , 700 , 750 , 800 Hz).

shaped acoustic devices such as a suction muffler to achieve high transmission loss in a target frequency range. The suggested design procedure is summarized as follows:

(1) Formulating a topology optimization problem using a finite element model: The objective function in Eq. (1) and the constraint in Eq. (2) are used with the interpolation function in Eq. (3). A non-design domain in a finite element model is properly declared for fluid passage.

(2) Solving the formulated topology optimization problem at several target frequencies and for several volume ratios, and obtaining optimal topologies: acoustic pressures are calculated by using the governing equations in Eqs. (5) and (6) and the boundary condition in Eq. (7). The transmission loss value at a target frequency and its sensitivity with respect to the design variables are calculated by using Eqs. (4) and (8), respectively. All of the design variables are updated through MMA [20]. Several optimal topologies are obtained.

(3) Determining an initial shape with design variables: on the basis of the optimal topologies, a potential best shape is determined by considering that uniform partitions facilitate acoustic device manufacturing. The lengths or thicknesses of the partitions are selected as design variables.

(4) Formulating a shape optimization problem with the initial shape: the objective function in Eq. (9) and constraint in Eq. (10) are used.

(5) Solving the formulated shape optimization problem and obtaining an optimal shape: the transmission loss value at a target frequency and its sensitivity are calculated by using the three-point method [19] and the difference equation in Eq. (11). All of the design variables are updated through MMA [20]. An optimal shape is obtained.

5. Conclusions

The advantages of topology optimization and shape optimization were combined to suggest a new suction muffler design method (two-step design process for an optimal suction muffler), which was experimentally validated. To maximize the transmission loss value at a target frequency, acoustical topol-

ogy and shape optimization problems were formulated. Two acoustical optimization problems were sequentially solved. First, creative optimal topologies were obtained at several target frequencies and for partition volume ratios. On the basis of the optimal topologies, a potential best shape was determined by considering that uniform partitions facilitate suction muffler manufacturing. Second, by selecting the best shape as an initial shape and solving the shape optimization problem, the optimal internal shape of a suction muffler was obtained. A comparison of the calculated transmission loss curves of the optimal shape mufflers and the measured transmission loss curves of manufactured acrylic mufflers supported the validity of our suggested method.

Acknowledgment

This research was supported by the Basic Science Research Program through the National Research Foundation of Korea (NRF) funded by the Ministry of Education, Science and Technology (No. 2010-0005299).

References

[1] I. J. C. Nunez, A. L. L. de Marqui, M. Cavaglieri and J. R. de F. Arruda, Investigating the transmission loss of compressor suction mufflers applying experimental and numerical methods, *Proceedings of the 19th International Compressor Engineering Conference*, West Lafayette, USA (2008) 1172-1-8.

[2] C. Svendsen, Acoustics of suction mufflers in reciprocating hermetic compressors, *Proceedings of the 17th International Compressor Engineering Conference*, West Lafayette , USA (2004) C029-1-7.

[3] K. Srioglu, A. R. Ozdemir, A. Kaya and E. Oguz, An experimental and numerical analysis of refrigerant flow inside the suction muffler of hermetic reciprocating compressor, *Proceedings of the 21th International Compressor Engineering Conference*, West Lafayette, USA (2012) 1184-1-9.

[4] J. Lee, K. H. An and I. S. Lee, Design of the suction muffler of a reciprocating compressor, *Proceedings of the 16th International Compressor Engineering Conference*, West Lafayette, USA (2002) C11-5.

[5] C. Svendsen and H. Møller, Acoustic optimization of suction mufflers in reciprocating hermetic compressors, *Proceedings of the Twelfth International Congress on Sound and Vibration*, Lisbon, Portugal (2005) CD-Rom.

[6] S. S. Gosavi, V. M. Juge and M. M. Nadgouda, Optimization of suction muffler using Taguchi's DOE Method, *Proceedings of the Eighteenth International Compressor Engineering Conference*, West Lafayette, USA (2006) C070-1-8.

[7] M. L. Munjal, *Acoustics of ducts and mufflers with application to exhaust and ventilation system design*, John Wiley and Sons, New York, USA (1987).

[8] A. Selamet and P. M. Radavich, The effect of length on the acoustic attenuation performance of concentric expansion chambers: an analytical, computational and experimental investigation, *Journal of Sound and Vibration*, 201 (4) (1997) 407-426.

[9] A. Selamet and Z. L. Ji, Acoustic attenuation performance of circular expansion chambers with extended inlet/outlet, *Journal of Sound and Vibration*, 223 (2) (1999) 197-212.

[10] A. Selamet, M. B. Xu, I. J. Lee and N. T. Huff, Analytical approach for sound attenuation in perforated dissipative silencers with inlet/outlet extensions, *Journal of the Acoustical Society of America*, 117 (4) (2005) 2078-2089.

[11] R. Barbieri and N. Barbieri, Finite element acoustic simulation based shape optimization of a muffler, *Applied Acoustics*, 67 (2006) 346-357.

[12] K. F. de Lima, A. Lenzi and R. Barbieri, The study of reactive silencers by shape and parametric optimization techniques, *Applied Acoustics*, 72 (2011) 142-150.

[13] M. P. Bendsøe and N. Kikuchi, Generating optimal topologies in optimal design using a homogenization method, *Computer Methods in Applied Mechanics and Engineering,* 71 (1988) 197-224.

[14] M. P. Bendsøe and O. Sigmund, *Topology optimization, Theory, Methods and Applications*, Springer, Berlin (2003).

[15] J. W. Lee and Y. Y. Kim, Topology optimization of muffler internal partitions for improving acoustical attenuation performance, *International Journal for Numerical Methods in Engineering*, 80 (2009) 455-477.

[16] J. W. Lee and G. W. Jang, Topology design of reactive mufflers for enhancing their acoustic attenuation performance and flow characteristics simultaneously, *International Journal for Numerical Methods in Engineering,* 91 (2012) 552-570.

[17] J. W. Lee and D. W. Choi, Topology optimization of suction muffler for noise attenuation, *Proceedings of the 21th International Compressor Engineering Conference*, West Lafayette, USA (2012) 1184-1-9.

[18] J. W. Lee and J. M. Lee, Forced vibro-acoustical analysis for a theoretical model of a passenger compartment with a trunk-Part I: Theoretical part, *Journal of Sound and Vibration*, 299 (2007) 900-917.

[19] T. W. Wu and G. C. Wan, Muffler performance studies using a direct mixed-body boundary element method and a three-point method for evaluating transmission loss, *Transaction of ASME: Journal of Vibration and Acoustics,* 118 (3) (1996) 479-484.

[20] K. Svanberg, The method of moving asymptotes: a new tool for structural optimization, *International Journal for Numerical Methods in Engineering,* 24 (1987) 359-373.

[21] L. H. Olesen, F. Okkels and H. Bruus. A high-level programming-language implementation of topology optimization applied to steady-state Navier-Stokes flow, *International Journal for Numerical Methods in Engineering,* 65 (7) (2006) 975-1001.

[22] *Comsol Multiphysics (Version 3.5)-scripting guide* (2008).

[23] J. W. Lee and Y. Y. Kim, Rigid body modeling issue in acoustical topology optimization, *Computer Methods in Applied Mechanics and Engineering*, 198 (2009) 1017-1030.

Jin Woo Lee is an Associate Professor of Mechanical Engineering at Ajou University since 2009. His research interests are in the area of vibrations, acoustics, topology optimization based design and fluid-structure interactions of microcantielvers for RF-MEMS and AFM. He received his Ph.D. in School of Mechanical and Aerospace Engineering from Seoul Notional University in South Korea in 2003. He worked with Samsung Electronics Company from 2003 to 2006 and studied as a post-doctoral research associate at Seoul National University from 2006 to 2007. From 2007 to 2009, he was a postdoctoral research associate of Mechanical Engineering at Purdue University, West Lafayette, IN, USA.

Kee Seung Oh received his B.S. degree in Division of Mechanical Engineering from Ajou University in South Korea in 2011. He is currently a combined master's and doctoral program candidate at the Multiscale Noise and Vibration Lab. in Ajou University. His research interests include design the noise reducing devices based on the topology optimization method.